Analytical Methods

RSC Publishing

PAPER

View Article Online
View Journal | View Issue



Cite this: *Anal. Methods*, 2013, **5**, 4126

# Liquid crystal based sensors for the detection of cholic acid

Sihui He,[a] Wenlang Liang,[b] Colleen Tanner,[b] Kung-Lung Cheng,[c] Jiyu Fang*[b] and Shin-Tson Wu*[a]

Received 2nd May 2013
Accepted 17th June 2013

DOI: 10.1039/c3ay40733k

**www.rsc.org/methods**

The concentration level of cholic acid is a biomarker for the early diagnosis of liver and intestinal diseases. We present a biosensor platform based on the anchoring transition of 4-cyano-4′-pentylbiphenyl (5CB) liquid crystals at surfactant-laden 5CB/aqueous interfaces for the detection of cholic acid (CA) in aqueous solution. In the biosensor platform, the competitive adsorption of CA at the surfactant-laden 5CB/aqueous interfaces can trigger a homeotropic-to-planar anchoring transition of the 5CB at the interface, which can be easily observed using a polarizing optical microscope. We find that the detection limit of the 5CB based biosensors for CA depends on the pH and ionic strength of the aqueous phase and the headgroup of the surfactants.

## 1 Introduction

Bile acids are physiologically important metabolites, which are synthesized in the liver as the end products of cholesterol metabolism and then secreted into the intestines. They play a critical role in the digestion and absorption of fats and fat-soluble vitamins through emulsification.[1] Bile acids are closely associated with liver and intestinal functions.[2] It has been shown that healthy individuals have the concentration of bile acids in the range of 4–10 μmol $L^{-1}$. While the concentration of bile acids for individuals with liver and intestinal diseases varies in the range from 67 to 376 μmol $L^{-1}$.[3] Thus, the concentration level of bile acids has long been used as a biomarker for the early diagnosis of liver and intestinal diseases.[4] Chromatography-mass spectrometry methods are commonly used for the detection of bile acids.[5–7] Although the precision of the methods in the detection of bile acids is high, they are time consuming and require expensive instruments. For the clinical diagnosis of liver and intestinal diseases, it is highly desirable to develop simple and rapid methods for the detection of bile acids. In recent years, chemical and optical sensors have been developed for the detection of bile acids.[8,9] For example, Koide *et al.* reported a chemical sensor based on an enzyme system for the detection of bile acids in aqueous solution.[8] Wu *et al.* fabricated an optical sensor based on molecularly imprinted hydrogels, which showed optical changes in response to the adsorption of bile acids in the hydrogels.[9]

Liquid crystals are anisotropic fluids, which have long-range orientational order.[10] The energy required to perturb the order of liquid crystals is very small. The changes of the surface in contact with liquid crystals often lead to the change in the local order. The local order induced by surface changes can extend over several tens of micrometers into the liquid crystals enabling the use of liquid crystals as an optical amplification probe for imaging self-assembled molecular systems[11–14] and biological cells.[15] Recently, surfactant-laden liquid crystal/aqueous interfaces have been developed to simply and rapidly detect enzymatic reactions,[16] ligand-receptor bindings,[17,18] DNA hybridizations,[19] and peptide–lipid membrane interactions[20] based on the anchoring transition of liquid crystals at the interfaces.

Cholic acid (CA) comprises 31% of the total bile acids produced in the liver. The concentration level of CA has been often used as an effective clinical biomarker for the diagnosis of liver and intestinal diseases.[4] In this paper, we report the use of 4-cyano-4′-pentylbiphenyl (5CB) liquid crystal films filled in the pores of TEM grids supported by polyimide-coated glass substrates as a sensor platform for the detection of CA in aqueous solution. The adsorption of surfactants at the 5CB/aqueous interface induces homeotropic anchoring of the 5CB at the interface. We find that the competitive adsorption of CA at the surfactant-laden 5CB/aqueous interface triggers a homeotropic-to-planar anchoring transition of the 5CB at the interface, providing a simple optical sign for the detection of CA with a polarizing optical microscope. The detection limit for CA depends on the pH and ionic strength of the aqueous phase and the headgroup of the surfactants.

[a]*College of Optics and Photonics, University of Central Florida, Orlando, FL 32816, USA. E-mail: swu@creol.ucf.edu*

[b]*Department of Materials Science and Engineering, University of Central Florida, Orlando, FL 32816, USA. E-mail: jfang@mail.ucf.edu*

[c]*Material and Chemical Research Laboratories, Industrial Technology Research Institute, Hsinchu, Taiwan*

## 2 Materials and methods

### 2.1 Materials

4-Cyano-4′-pentylbiphenyl (5CB), cholic acid (CA), lithocholic acid (LCA), sodium dodecyl sulfate (SDS), tetra(ethylene glycol) monododecyl ether ($C_{12}E_4$), and dodecyltrimethylammonium bromide (DTAB) were obtained from Sigma-Aldrich (St. Louis, MO). Cholyl-lysyl-fluorescein (CLF) was purchased from BD Biosciences (Woburn, MA). All chemicals were used without further purification. Water used in our experiments was purified using an Easypure II system (18.2 MΩ cm and pH 5.7). Phosphate buffered saline (PBS) solution was from Sigma-Aldrich (St. Louis, MO). Polyimide coated glass substrates used for inducing a homeotropic anchoring of liquid crystals were purchased from AWAT PPW (Warsaw, Poland). Glass microscopy slides were from Fisher Scientific. Copper TEM grids (18 μm thickness, 285 μm grid spacing, and 55 μm bar width) were obtained from Electron Microscopy Sciences (Hatfield, PA).

### 2.2 Preparation of liquid crystal films

Copper TEM grids were cleaned with ethanol and then heated at 110 °C for 24 h. The cleaned TEM grids were placed on polyimide-coated glass substrates. One microliter of 5CB was filled in the pores of the TEM grids supported by the polyimide-coated glass substrates. The excess 5CB was removed by using a capillary tube, leading to the formation of 5CB films in the pores of the grids. The 5CB films were then immersed in aqueous solution containing surfactants (SDS, $C_{12}E_4$, and DTAB). The adsorption of these surfactants leads to the formation of a surfactant-laden 5CB/aqueous interface.

### 2.3 Optical observation

The optical texture of the 5CB films filled in the pores of the TEM grids was examined with a polarizing optical microscope (BX 40, Olympus) in transmission mode. All optical microscopy images were taken with a digital camera (C2020 Zoom, Olympus) mounted on the polarizing optical microscope at room temperature. Fluorescence microscopy images were acquired with a confocal fluorescence microscope (Zeiss TCS SP5MP) with 488 nm excitation from an $Ar^+$ laser.

## 3 Results and discussion

The chemical structures of 5CB, CA, LCA, SDS, DTAB, $C_{12}E_4$ and CLF are shown in Fig. 1. 5CB is a nematic LC with a crystal-to-nematic transition temperature at 24 °C and a nematic-to-isotropic transition temperature at 35 °C. CA has a quasi-planar steroid ring system with four hydrogen atoms at the convex face and three hydroxyl groups at the concave face. A carboxylic acid group is linked to the steroid ring through a short alkyl chain. CLF is a fluorescent CA. SDS, DTAB, and $C_{12}E_4$ have the same hydrophobic tail but different headgroups, which were used to induce surfactant-laden 5CB/aqueous interfaces.

Fig. 2a shows a polarizing optical microscopy image of 5CB films filled in the pores of TEM grids supported by polyimide-coated glass substrates after being immersed in aqueous solution containing 1.8 mM SDS for 30 min at pH 5.8. The adsorption of SDS at the 5CB/aqueous interface leads to the formation of a SDS-laden 5CB/aqueous interface. The dark appearance shown in Fig. 2a indicates a homeotropic anchoring of the 5CB at the SDS-laden 5CB/aqueous interface. The homeotropic anchoring is a result of the interaction between the SDS and the 5CB at the interface. CA was dissolved in NaOH aqueous solution. When a certain amount of CA solution is added into the aqueous phase side of the SDS-laden 5CB/aqueous interface, we find that the optical appearance of the 5CB films in the pores of TEM grids changes from a dark appearance to bright domains within 5 min (Fig. 2b). The appearance of the bright domains reflects a continuous change in the orientation of the 5CB from a homeotropic anchoring at the polyimide-coated glass substrate to a planar anchoring at the SDS-laden 5CB/aqueous interface.[16]

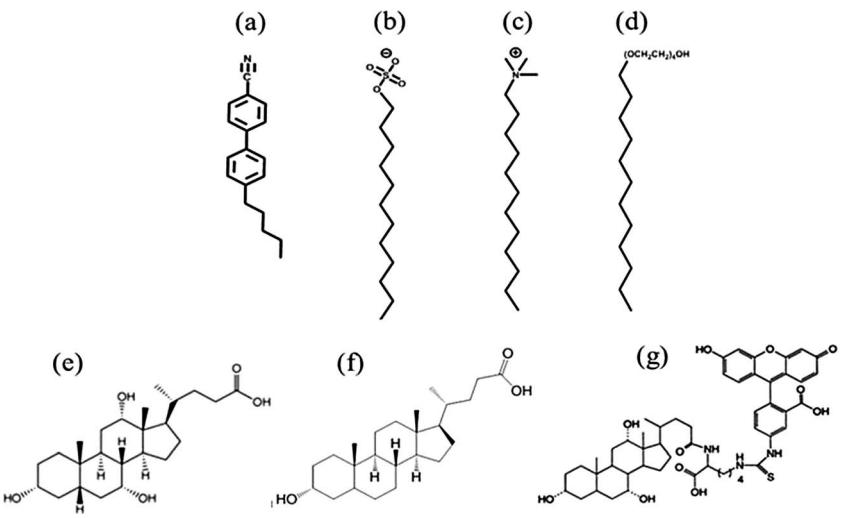


**Fig. 1** Chemical structures of 5CB (a), SDS (b), DTAB (c), $C_{12}E_4$ (d), CA (e), LCA (f), and CLF (g).

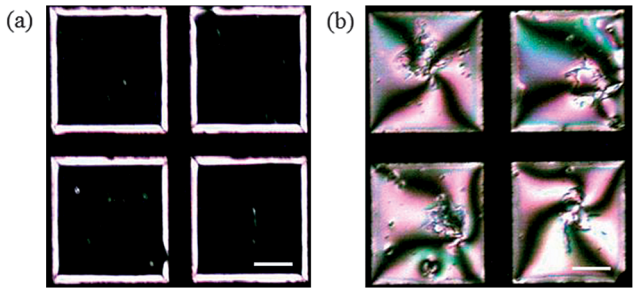


**Fig. 2** Polarizing optical microscopy images of a SDS-laden 5CB/aqueous interface before (a) and after (b) being exposed to 24 μM CA solution. Scale bar: 145 μm.

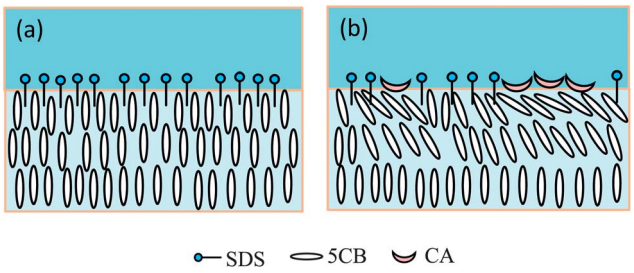


**Fig. 4** Schematic illustrations of the anchoring transition of the 5CB at a SDS-laden 5CB/aqueous interface before (a) and after (b) being exposed to CA solution.

It is known that bile acids are biological surfactants which competitively adsorb onto the lipid interface of gastric emulsions when they enter the duodenum.[21] Several reports have shown that bile acids can disrupt the packing of the lipids adsorbed at the oil–water interface through the competitive adsorption.[22,23] By using CLF (a fluorescent CA, see Fig. 1g), we confirm that the anchoring transition of the 5CB at the SDS-laden 5CB/aqueous interface is a result of the competitive adsorption of CA at the interface. After addition of CLF into the aqueous phase side of the SDS-laden 5CB/aqueous interface, the optical appearance of the 5CB films in the pores of the TEM grids changes from a uniform dark field to bright domains (Fig. 3a), suggesting a homeotropic-to-planar anchoring transition of the 5CB at the interface. The corresponding confocal fluorescent image shows a strong fluorescence from the interface (Fig. 3b), confirming the competitive adsorption of CLF at the interface. Thus, it is reasonable for us to assume that the packing of the SDS at the 5CB/aqueous interface is disrupted by the competitive adsorption of CA. Since CA is an amphipathic molecule, we expect that the CA adsorbs at the 5CB/aqueous interface with its hydrophobic convex face toward the 5CB phase and its hydrophilic concave face toward the aqueous phase. The disruption of the SDS at the 5CB/aqueous interface by the competitive adsorption of CA triggers the anchoring transition of the 5CB at the interface (Fig. 4).

The anchoring transition of the 5CB at the SDS-laden 5CB/aqueous interface triggered by the competitive adsorption of CA is concentration dependent. Thus, by observing the anchoring transition of the 5CB at the SDS-laden 5CB/aqueous interface with a polarizing optical microscope, we will be able detect the concentration of CA in aqueous solution. The minimum concentration (defined as the detection limit) of CA required to trigger the anchoring transition of the 5CB at the SDS-laden 5CB/aqueous interface is found to depend on the pH of the aqueous phase (Fig. 5). When the pH value varies from 3.5 to 5.0, the detection limit for CA remains nearly unchanged (~12 μM). However, when the pH is above 5.0, the detection limit rapidly increases and reaches to ~170 μM at pH 7.5. The pH dependent detection limit is likely associated with the ionization of CA. The p$K_a$ of CA is measured to be ~5.0.[24] When the pH of the aqueous phase is above 5.0, the carboxylic acid group of CA is expected to be ionized. Thus, the repulsive force between the negatively charged CA and the negatively charged SDS reduces the adsorption of CA at the 5CB/aqueous interface, leading to the increased detection limit of the SDS-laden 5CB/aqueous interface for CA.

Furthermore, we study the effect of surfactant headgroups on the detection limit by forming cationic DTAB- and nonionic $C_{12}E_4$-laden 5CB/aqueous interfaces. The adsorption of both DTAB and $C_{12}E_4$ at the 5CB/aqueous interface induces a homeotropic anchoring of the 5CB at the interface, which is consistent with the results reported in the literature.[25] When CA is added to the aqueous phase side of the DTAB- and $C_{12}E_4$-laden 5CB/aqueous interfaces, we find no anchoring transition of the 5CB at the interfaces if the pH of the aqueous phase is above 5.0 (Fig. 6a and c). This result suggests that the anionic

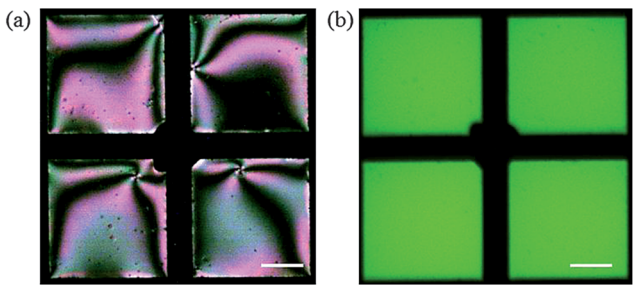


**Fig. 3** Polarizing (a) and fluorescence (b) microscopy images of a SDS-laden 5CB/aqueous interface after being exposed to 0.25 μM CLF solution. Scale bar: 145 μm.

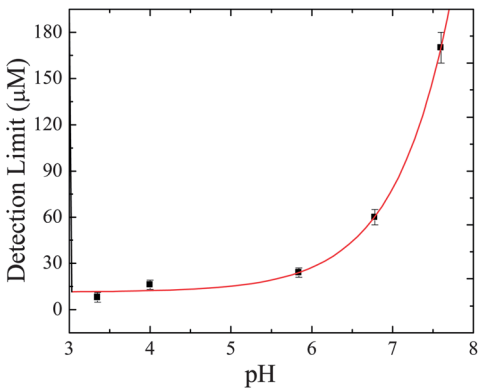


**Fig. 5** Detection limit of a SDS-laden 5CB/aqueous interface for CA as a function of pH values. The data points were obtained from three samples.

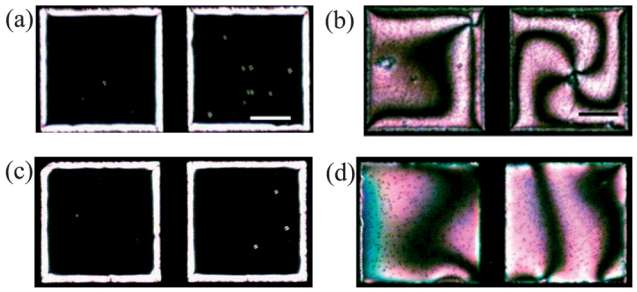


**Fig. 6** Polarizing optical microscopy images of DTAB (a and b) and $C_{12}E_4$ (c and d) laden 5CB/aqueous interfaces before (a and c) and after (b and d) being exposed to 90 and 200 μM CA solution at pH 3.5, respectively. Scale bar: 145 μm.

CA is unable to disrupt the packing of the cationic DTAB and the nonionic $C_{12}E_4$ at the 5CB/aqueous interfaces. For the cationic DTAB-laden 5CB/aqueous interface, the anionic CA may adsorb on the cationic DTAB layer through electrostatic interaction, rather than disrupt the DTAB at the 5CB/aqueous interface. However, when the pH of the aqueous phase is lower than 5.0, the anchoring transition of the 5CB at the DTAB- and $C_{12}E_4$-laden 5CB/aqueous interfaces is observed after being exposed to CA solution (Fig. 6b and d). For example, the detection limit of the DTAB- and $C_{12}E_4$-laden 5CB/aqueous interfaces for CA at pH 3.5 is found to be ~120 μM and ~200 μM, respectively (Fig. 7a). The different detection limits of surfactant-laden 5CB/aqueous interfaces for CA at the same pH value may reflect the difference in the affinity and packing density of the surfactants at the 5CB/aqueous interface. It has been shown that DTAB is more efficient than SDS in reducing the interfacial tension, which suggests that DTAB is more surface active than SDS.[26] Therefore, we can expect that the DTAB at the 5CB/aqueous interface is more difficult to be disrupted by CA, compared to the SDS. Thus, the detection limit of the DTAB-laden 5CB/aqueous interface is expected to be higher than that of the SDS-laden 5CB/aqueous interface, which is consistent with our results. For the $C_{12}E_4$-laden 5CB/aqueous interface, the detection limit for CA at pH 3.5 reaches to ~200 μM, which is two times higher than that of the DTAB-laden 5CB/aqueous interface. It has been shown that the packing density of the nonionic $C_{12}E_4$ at the air/aqueous interface is higher than that of the cationic DTAB and the anionic SDS.[27] Thus, the densely packed $C_{12}E_4$ at the 5CB/aqueous interface is more difficult to be disrupted by CA, compared to the loosely packed DTAB and SDS at the 5CB/aqueous interface, leading to the highest detection limit for CA shown in Fig. 7a.

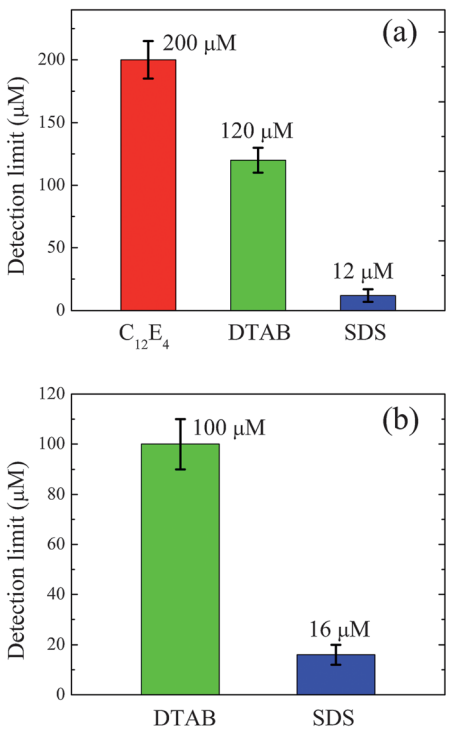


**Fig. 7** Detection limit of surfactant-laden 5CB/aqueous interfaces for CA in aqueous solution with an ionic strength of 2 mM at pH 3.5 (a) and PBS with an ionic strength of 172 mM at pH 7.5 (b).

We further carried out the detection of CA in phosphate buffered saline (PBS) solution with the ionic strength of 172 mM and the pH of 7.5. The detection limit for CA in PBS solution is ~16 μM for the SDS-laden 5CB/aqueous interface and ~100 μM for the DTAB-laden 5CB/aqueous interface, respectively (Fig. 7b). In addition, no anchoring transition of the 5CB at the $C_{12}E_4$-laden interface is observed after addition of CA in PBS solution. The detection limit (~16 μM) of the SDS-laden 5CB/aqueous interfaces in PBS solution with an ionic strength of 172 mM is much lower than that in NaOH aqueous solution with an ionic strength of 2 mM at the same pH 7.5. The effect of the ionic strength on the surface anchoring of the 5CB at the 5CB/aqueous interface has been reported in the literature,[28] which shows that the increase of the ionic strength of the aqueous phase favors for a homeotropic anchoring of the 5CB at the interface due to the formation of an electrical double layer on the 5CB phase side of the 5CB/aqueous interface. However, the effect of the electrical double layer on the anchoring of the 5CB at the interface cannot explain the decreased detection limit of the SDS-laden 5CB/aqueous interface in PBS solution. We infer that the decreased detection limit for CA in PBS solution may be a result of the charge screening of the anionic SDS at the 5CB/aqueous interface and the anionic CA in the aqueous phase at pH 7.5. Thus, the screening of the electrostatic interaction at high ionic strengths promotes the CA to penetrate into the SDS layer and disrupt the packing of SDS at the 5CB/aqueous interface. Consequently, the decreased detection limit for CA in PBS solution is observed.

In biological fluids, ascorbic acid (AA) coexists with bile acids in a high concentration. It has been shown that AA is a major interfering specie in the detection of bile acids. We find that there is no anchoring transition of the 5CB at the SDS-laden 5CB/aqueous interface when 50 μM AA is added into PBS solution (Fig. 8a), suggesting that AA is unable to disrupt the SDS at the 5CB/aqueous interface. Furthermore, we measure the concentration of CA required to trigger the anchoring transition of the 5CB at the SDS-laden 5CB/aqueous interface in the presence of 50 μM AA and find that the detection limit (16 μM) for CA remains unchanged (Fig. 8b), suggesting that we are able to selectively detect CA in the presence of AA. We would like to point out that lithocholic acid (LCA) (Fig. 1f), a secondary bile

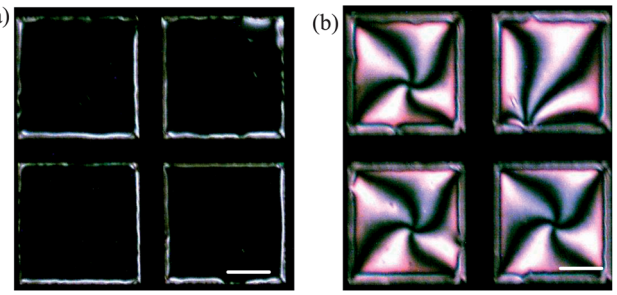


**Fig. 8** Polarizing optical microscopy images of SDS-laden 5CB/aqueous interfaces after being exposed to PBS solution containing 50 μM AA (a) and 16 μM CA and 50 μM AA (b) at pH 7.5. Scale bar: 145 μm.

acid, is also able to trigger the anchoring transition of the 5CB at the SDS-laden 5CB/aqueous interface at a concentration of ~10 μM. But, LCA only comprises less than 0.5% of the total bile acids. The detection limit of the SDS-laden 5CB/aqueous interface for CA is higher than that of chromatography-mass spectrometry methods (2.4 pM) (ref. 7) and molecularly imprinted hydrogel based sensors (10 pM),[9] but comparable with that of electrochemical[8] and colorimetric[29] sensors. The advantage of the liquid crystal based sensing platform for the detection of CA is simple and fast without the need for expensive instruments.

## 4 Conclusion

The concentration level of CA is a clinical biomarker for the early diagnosis of liver and intestinal diseases because individuals suffering these diseases have sharply increased concentration of CA at micromolar levels. We have used a biosensor platform based on the anchoring transition of the 5CB at the surfactant-laden 5CB/aqueous interface for the detection of CA in aqueous solution. The competitive adsorption of CA at the surfactant-laden 5CB/aqueous interface can trigger a homeotropic-to-planar anchoring transition of the 5CB at the interface, providing a simple optical sign for the detection of CA. The detection limit of surfactant-laden 5CB/aqueous interfaces for CA can be changed by altering the pH and ionic strength of the aqueous phase and the headgroup of the surfactants.

## Acknowledgements

The authors acknowledge Drs Kevin Belfield and Ciceron Yanez for their assistance with confocal fluorescence microscopy. This work was supported by the ITRI Display Technology Center (Taiwan) and the US National Science Foundation (CBET 0931778).

## References

1 A. F. Hofmann and L. R. Hagey, *Cell. Mol. Life Sci.*, 2008, **65**, 2461.
2 C. Degirolamo, S. Modica, G. Palasciano and A. Moschetta, *Trends Mol. Med.*, 2011, **17**, 564.
3 K. Rani, P. Garg and C. S. Pundir, *Anal. Biochem.*, 2004, **332**, 32.
4 W. J. Griffiths and J. Sjövall, *J. Lipid Res.*, 2010, **51**, 23.
5 B. Alme, A. Bremmelgaard, J. Sjövall and P. Thomassen, *J. Lipid Res.*, 1977, **18**, 339.
6 A. H. Que, T. Konse, A. G. Baker and M. V. Novotny, *Anal. Chem.*, 2000, **72**, 2703.
7 S. Perwaiz, B. Tuchweber, D. Mignault, T. Gilat and I. M. Yousef, *J. Lipid Res.*, 2001, **42**, 114.
8 S. Koide, N. Ito and I. Karube, *Biosens. Bioelectron.*, 2007, **22**, 2079.
9 Z. Wu, X. Hu, C. Tao, Y. Li, J. Liu, C. Yang, D. Shen and G. Li, *J. Mater. Chem.*, 2008, **18**, 5452.
10 P. G. De Gennes, *The physics of liquid crystals*, Clarendon, Oxford, 1974.
11 J. Y. Fang, U. Gehlert, R. Shashidhar and C. M. Knobler, *Langmuir*, 1999, **15**, 297.
12 Y. Zhao, N. Mahajan, R. Lu and J. Y. Fang, *Proc. Natl. Acad. Sci. U. S. A.*, 2005, **102**, 7438.
13 I. H. Lin, M. V. Meli and N. L. Abbott, *J. Colloid Interface Sci.*, 2009, **336**, 90.
14 A. D. Price and D. K. Schwartz, *J. Phys. Chem. B*, 2007, **111**, 1007.
15 J. Y. Fang, W. Ma, J. V. Selinger and R. Shashidhar, *Langmuir*, 2003, **19**, 2865.
16 J. M. Brake, M. K. Daschner, Y.-Y. Luk and N. L. Abbott, *Science*, 2003, **302**, 2094.
17 D. Hartono, C. Xue, K. Yang and L. L. Yung, *Adv. Funct. Mater.*, 2009, **19**, 3574.
18 L. N. Tan, P. J. Bertics and N. L. Abbott, *Langmuir*, 2011, **27**, 1419.
19 A. D. Price and D. K. Schwartz, *J. Am. Chem. Soc.*, 2008, **130**, 8188.
20 Q. Z. Hu and C. H. Jang, *Analyst*, 2012, **137**, 567.
21 M. C. Carey, *Annu. Rev. Physiol.*, 1983, **45**, 651.
22 B. S. Chu, G. T. Rich, M. J. Ridout, R. M. Faulks, N. S. J. Wickham and P. J. Wilde, *Langmuir*, 2009, **25**, 9352.
23 A. Torcello-Gómez, J. Maldonado-Valderrama, A. Martín-Rodríguez and D. J. McClements, *Soft Matter*, 2011, **7**, 6167.
24 A. Fini and A. Roda, *J. Lipid Res.*, 1987, **28**, 755.
25 J. M. Brake, A. D. Mezera and N. L. Abbott, *Langmuir*, 2003, **19**, 6436.
26 B. Sohrabi, H. Gharibi, B. Tajik, S. Javadian and M. Hashemianzadeh, *J. Phys. Chem. B*, 2008, **112**, 14869.
27 C. T. Hsu, M. J. Shao and S. Y. Lin, *Langmuir*, 2000, **16**, 3187.
28 R. J. Carlton, J. K. Gupta, C. L. Swift and N. L. Abbott, *Langmuir*, 2012, **28**, 31.
29 M. Y. Qureshi, S. M. Smith and G. M. Murphy, *J. Clin. Pathol.*, 1984, **37**, 317.

 